

Identifying key genes associated with acute myocardial infarction

Ming Cheng, MM, Shoukuan An, MD, Junquan Li, MD*

Abstract

Background: This study aimed to identify key genes associated with acute myocardial infarction (AMI) by reanalyzing microarray data.

Methods: Three gene expression profile datasets GSE66360, GSE34198, and GSE48060 were downloaded from GEO database. After data preprocessing, genes without heterogeneity across different platforms were subjected to differential expression analysis between the AMI group and the control group using metaDE package. $P < .05$ was used as the cutoff for a differentially expressed gene (DEG). The expression data matrices of DEGs were imported in ReactomeFIViz to construct a gene functional interaction (FI) network. Then, DEGs in each module were subjected to pathway enrichment analysis using DAVID. MiRNAs and transcription factors predicted to regulate target DEGs were identified. Quantitative real-time polymerase chain reaction (RT-PCR) was applied to verify the expression of genes.

Result: A total of 913 upregulated genes and 1060 downregulated genes were identified in the AMI group. A FI network consists of 21 modules and DEGs in 12 modules were significantly enriched in pathways. The transcription factor-miRNA-gene network contains 2 transcription factors FOXO3 and MYBL2, and 2 miRNAs hsa-miR-21-5p and hsa-miR-30c-5p. RT-PCR validations showed that expression levels of FOXO3 and MYBL2 were significantly increased in AMI, and expression levels of hsa-miR-21-5p and hsa-miR-30c-5p were obviously decreased in AMI.

Conclusion: A total of 41 DEGs, such as *SOCS3*, *VAPA*, and *COL5A2*, are speculated to have roles in the pathogenesis of AMI; 2 transcription factors *FOXO3* and *MYBL2*, and 2 miRNAs hsa-miR-21-5p and hsa-miR-30c-5p may be involved in the regulation of the expression of these DEGs.

Abbreviations: AMI = acute myocardial infarction, CTGF = connective tissue growth factor, FI = functional interaction, H-FABP = heart fatty acid binding protein, RT-PCR = real-time PCR.

Keywords: acute myocardial infarction, differentially expressed genes, gene functional interaction, pathway enrichment analysis, transcription factor-miRNA-gene network

1. Introduction

Acute myocardial infarction (AMI) is the world's leading cause of morbidity and mortality. A ruptured atherosclerotic plaque, causing thrombosis and occlusion of the coronary artery, is widely accepted for the occurrence of an AMI. Early reperfusion of the occluded artery after MI, including primary percutaneous

coronary intervention (PCI) or thrombolytic therapy, will improve long-term prognosis of patients. Thrombolytic therapy has become the standard therapy for AMI since 1980s.^[1] Recently, primary PCI seems to be more effective than fibrinolytic therapy in acute ST-segment elevation myocardial infarction.^[2] However, approximately one-third of eligible patients failed to receive early reperfusion therapy because of late presentation.^[3,4] Thus, an early diagnosis may benefit the survival remarkably.

Cardiac troponins (T/I) have been long considered as the "gold standard" biomarkers for early detection of AMI.^[5,6] However, more sensitive and potent makers are preferred. Mccann et al^[7] have proposed that heart fatty acid binding protein (H-FABP) is superior than cardiac troponin T. Several circulating microRNAs (miR-208a, miR-499, and miR-1) have also been recommended as potential biomarkers for early diagnosis of myocardial infarction.^[8-10] Here, using 3 public gene expression profile datasets, we attempted to identify novel genes that may be useful for the early detection of AMI by bioinformatics methods.

2. Materials and methods

2.1. Source of microarray data

Three gene expression profile datasets GSE66360, GSE34198, and GSE48060 were downloaded from GEO (Gene Expression Omnibus, <http://www.ncbi.nlm.nih.gov/geo/>) database. The samples included in each dataset and annotation platform are listed in Table 1.

Editor: Alfons Lawen.

MC and SA should be regarded as cofirst authors.

Funding/support: This study was supported by Youth Science Foundation of Heilongjiang Province (No.: QC2013C116) and Sub-project of National Hi-tech Research and Development Plan Foundation (No.: 2007AA021907).

The authors declare that they have no competing interests.

Department of Cardiac Surgery, The Second Affiliated Hospital of Harbin Medical University, Nangang, Harbin, Heilongjiang, People's Republic of China.

* Correspondence: Junquan Li, Department of Cardiac Surgery, The Second Affiliated Hospital of Harbin Medical University, Nangang, Harbin 150086, Heilongjiang, People's Republic of China (e-mail: LJQ666@163.com).

Copyright © 2017 the Author(s). Published by Wolters Kluwer Health, Inc. This is an open access article distributed under the terms of the Creative Commons Attribution-Non Commercial-No Derivatives License 4.0 (CCBY-NC-ND), where it is permissible to download and share the work provided it is properly cited. The work cannot be changed in any way or used commercially without permission from the journal.

Medicine (2017) 96:42(e7741)

Received: 28 December 2016 / Received in final form: 29 June 2017 /

Accepted: 17 July 2017

<http://dx.doi.org/10.1097/MD.0000000000007741>

Table 1**Information on platform and study subjects in each gene expression profile dataset.**

	AML sample count	Control sample count	Platforms
GSE66360	49	50	Affymetrix Human Genome U133 Plus 2.0 Array
GSE34198	49	48	Illumina human-6 v2.0 expression beadchip
GSE48060	31	21	Affymetrix Human Genome U133 Plus 2.0 Array

2.2. Microarray data preprocessing

For the raw data in GSE66360 and GSE34198, they were first subjected to background correction and quantile normalization using the Affy package of R/Bioconductor.^[11] For data in GSE34198, the Limma package of R/Bioconductor was used for background correction, normalization between arrays, and microarray data condensation.

2.3. Heterogeneity test and screening of characteristic genes

First, heterogeneity of each gene across different platforms was examined by measuring τ^2 , Q value, and Q P value using MetaDE.ES function; τ^2 of 0 and Q pval >0.05 indicate no heterogeneity. Next, genes without heterogeneity were subjected to differential expression analysis of their expression levels between the AMI group and the control group using metaDE package; $P < .05$ was used as the cutoff for a differentially expressed gene (DEG). The \log_2FC (fold change) value of a gene in each dataset was further calculated, with $\log_2FC > 0$ as upregulated and $\log_2FC < 0$ as downregulated.

2.4. Pathway enrichment analysis of DEGs

The screened DEGs were submitted to DAVID (v6.8, Database for Annotation, Visualization and Integrated Discovery, <https://david.ncifcrf.gov/>) to examine the pathways in which these genes were enriched based on the KEGG database (Kyoto Encyclopedia of Genes and Genomes) ($P < .05$).^[12]

2.5. Construction of gene functional interaction network

The expression data matrix of DEGs was submitted to ReactomeFIViz to investigate gene–gene interaction based on known human pathway data.^[13] ReactomeFIViz first constructs a functional interaction (FI) network by merging interactions extracted from human curated pathways and the average Pearson correlation coefficient among genes involved in the same FIs are also calculated as weights for edges (i.e., FIs) in the whole FI network; next, using MCL (Monte Carlo Localization) graph clustering algorithm, subnetworks for a list of selected network modules were generated based on module size and average correlation. The FI network was finally visualized using Cytoscape 2.8.0 (National Institute of General Medical Sciences of the National Institutes of Health).^[14]

2.6. Prediction of AMI-related microRNAs and construction of miRNA-gene network

First, microRNAs related to AMI were identified from the miR2disease database (<http://www.mir2disease.org/>). Next, the target genes that have been experimentally validated were downloaded from Mirwalk2,^[15] which were further compared with the DEGs screened above. Next, these miRNAs and their target DEGs were used to construct a miRNA-gene network.

2.7. Prediction of transcription factor-miRNA-gene network

Transcription factors of the DEGs in the miRNA-gene network constructed above were predicted using a Cytoscape plug-in iRegulon,^[16] which includes gene-transcription factor pairs in Transfac, Jaspar, Encode, etc. Minimum identity between orthologous genes was 0.05 and maximum false discovery rate on motif similarity: 0.001. The transcription factors predicted with normalized enrichment score (NES) >3 were retained.

2.8. Validation of DEGs

A total of 16 blood samples, including 8 normal control and 8 AMI blood samples, were collected from the Second Affiliated Hospital of Harbin Medical University to verify the expression levels of *FOXO3*, *MYBL2*, hsa-miR-30c-5p, and hsa-miR-21-5p identified in this study using quantitative real-time polymerase chain reaction (RT-PCR). Total RNAs were isolated using TRI pure LS Reagent Blood RNA Extraction Kit (Biotek, Lot: RP1102, Beijing, China). Then, 4 μ g of total RNA was utilized miRNA reverse transcription using Rayscript cDNA Synthesis Kit (GCK8030, GENEray, Shanghai, China) with neck-loop primers instead of Oligo (dT). Amplification of miRNA was carried out on a ViiA7 real-time PCR instrument (ABI, Foster City, CA) using the following system: 50°C for 3 minutes, then 40 cycles of 95°C for 3 minutes, 95°C for 10 seconds, and 60°C for 30 seconds. Meanwhile, 0.5 μ g of total RNA was applied to mRNA reverse transcription using Rayscript cDNA Synthesis Kit (GCK8030, GENEray, Shanghai, China). Amplification of mRNA was performed using the following system: 95°C for 2 minutes, then 40 cycles of 95°C for 15 seconds, 60°C for 20 seconds, and 72°C for 20 seconds. Primers of RNAs are tabulated in Table 2. GAPDH was

Table 2**Primers of genes determined by quantitative real-time PCR.**

Primers	Sequences
FOXO3 -F	TGATGGGCTGACTGAAAAC
FOXO3-R	AGATGAAGGTCCGAACACC
MYBL2 -F	GAGGAAAACAGTGAGGAGGA
MYBL2-R	GCAGGGATGAGGAGGTTAG
GAPDH-F	GGACCTGACCTGCCGTCTAG
GAPDH -R	GTAGCCCAAGGATGCCCTTGA
hsa-miR-21-5p-neck-loop	CCTGTTGTCTCCAGCCACAAAAGAGC ACAATATTTTCAGGAGACAACAGGTCAACA
hsa-miR-21-5p probe	FAM-TTCAGGAGACAACAGG-MGB
hsa-miR-21-5p-F	CAGCCACAAAAGAGCACAAAT
hsa-miR-21-5p-R	GGGGGTAGCTTATCAGACTGA
hsa-miR-30c-5p-neck-loop	CCTGTTGTCTCCAGCCACAAAAGAGC ACAATATTTTCAGGAGACAACAGGCTGAG
hsa-miR-30c-5p probe	FAM-TTCAGGAGACAACAGG-MGB
hsa-miR-30c-5p-F	CAGCCACAAAAGAGCACAAAT
hsa-miR-30c-5p-R	GGGGGTGTAACATCCTACACT
5S-neck-loop	CCTGTTGTCTCCAGCCACAAAAGAGC CACAATATTTTCAGGAGACAACAGGAAAAGCCTA
5S probe	FAM-TTCAGGAGACAACAGG-MGB
5S-F	CAGCCACAAAAGAGCACAAAT
5S-R	GAGACCGCTGGGAATAC

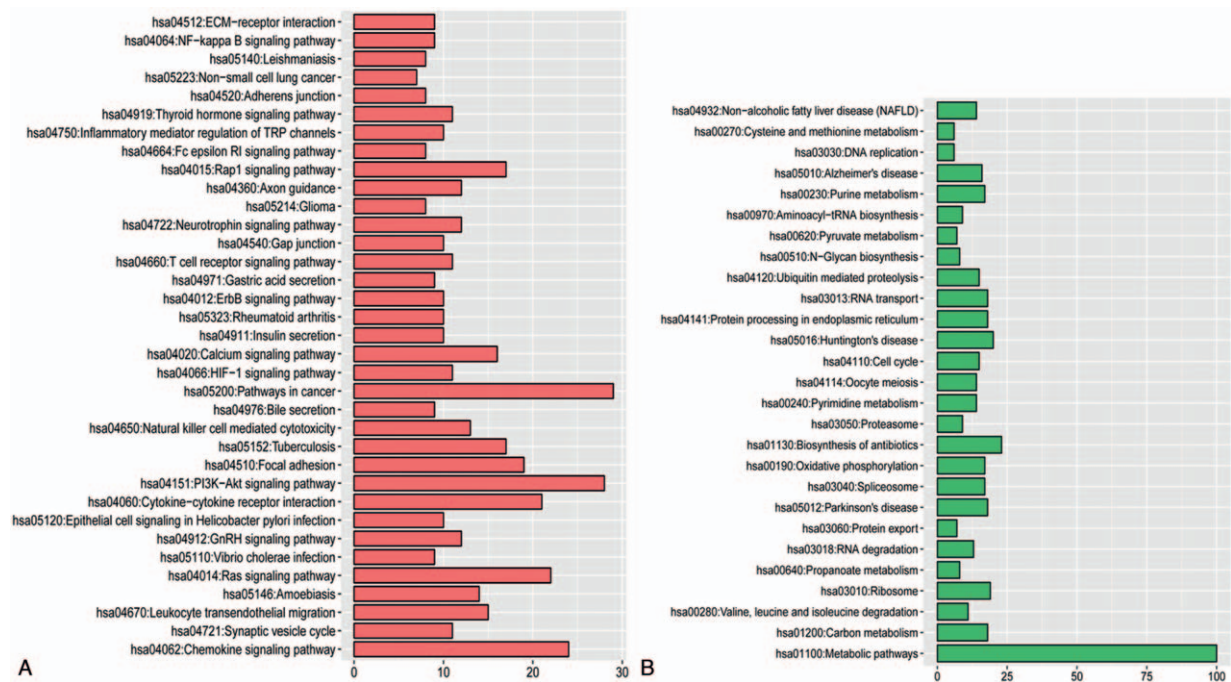


Figure 1. Pathway enrichment analysis of differentially expressed genes A, pathways enriched by the upregulated genes; B, pathways enriched by the downregulated genes.

utilized as the internal control for mRNA evaluation, and 5S was utilized as the internal reference for miRNA evaluation. The ethics committee of the Second Affiliated Hospital of Harbin Medical University approved this study, and informed written consents were obtained from the included subjects.

3. Results

3.1. Screening of candidate characteristic genes

According to the analytical results, a total of 913 upregulated genes and 1060 downregulated genes were identified in the AMI group compared with the control group. Then, KEGG enrichment analyses for upregulated and downregulated genes were carried out. The enrichment results performed that the upregulated genes and downregulated genes were enriched in 35 and 27 KEGG pathways, respectively (Fig. 1).

3.2. Construction of FI network and pathway enrichment analysis

On the basis of the expression data matrices, a FI network was constructed, which contained 249 nodes forming 1071 interaction pairs (Fig. 2). The network includes 21 modules, of which 12 modules had Pearson correlation coefficient > 0.9 .

KEGG pathway enrichment of DEGs in each module shows that DEGs in Module 1 were significantly enriched in 38 KEGG pathways, such as DEGs in Module 5 and 13 were enriched in 7 pathways each; DEGs in Module 20 were enriched in 6 pathways; DEGs in Module 3 were enriched in 4 pathways; DEGs in Module 9 were enriched in 3 pathways, such as hsa04630: Jak-STAT signaling pathway; DEGs in Module 6 and 14 were enriched in 2 pathways each; DEGs in Module 2, 4, 7, 11, and 19 were enriched in 1 pathway each (Table 3).

3.3. Construction of miRNA-gene network

The miRNA-gene network consists of 9 miRNAs (hsa-miR-21, hsa-miR-133, hsa-miR-29, hsa-miR-30c, hsa-miR-1, hsa-miR-133a, hsa-miR-133b, hsa-miR-208, hsa-miR-499) and 191 genes, forming 213 miRNA-gene pairs (Fig. 3). Among the DEGs in this network, 28 were also found in the FI network.

3.4. Prediction of transcription factor-miRNA-gene network

The transcription factor-miRNA-gene network contains 40 DEGs, including 14 upregulated genes (*CBX4*, *CCR1*, *COL5A2*, *FGF12*, *FKBP5*, *IGF1R*, *LAMP2*, *MEGF9*, *MMP2*, *OTUD1*, *TGFB2*, *NDEL1*, *UBN1*, and *VAPA*) and 26 downregulated genes (*ADNP*, *CD47*, *CDK6*, *CKAP5*, *CLIP4*, *DAAMI*, *DOCK10*, *FAM20B*, *FAM3C*, *FBXL17*, *FOXN2*, *HPS5*, *LCORL*, *MTMR9*, *NBEA*, *NEK1*, *PER3*, *PHACTR2*, *POLR3B*, *PRRC1*, *SCRN1*, *SEC63*, *SLK*, *SOCS5*, *TET1*, and *ZBTB20*), 2 upregulated transcription factors *FOXO3* and *MYBL2*, and 2 downregulated miRNAs hsa-miR-21-5p and hsa-miR-30c-5p (Fig. 4).

3.5. Experimental validations of DEGs

To further confirm our identifications, the expression levels of *FOXO3* and *MYBL2* and 2 miRNAs hsa-miR-21-5p and hsa-miR-30c-5p were determined in AMI patients and normal controls. The RT-PCR results presented that the relative mRNA expression levels of *FOXO3* and *MYBL2* were significantly increased in AMI patients compared with the normal controls (Fig. 5A and B). Meanwhile, the expression levels of hsa-miR-30c-5p and hsa-miR-21-5p were significantly decreased in AMI patients compared with the normal controls (Fig. 5C and D).

Table 3**Pathway enrichment analysis of differentially expressed genes in the modules of the gene functional interaction network.**

Module ID	Pathway term	Gene count	P	Genes	FDR
Module1	hsa04740:Olfactory transduction	8	4.99E-06	<i>OR10A5, OR13C4, OR10A3, OR11A1, PRKACA, PRKACB, OR8G1, OR1G1</i>	0.0050308
	hsa04020: Calcium signaling pathway	6	1.66E-05	<i>ADCY4, ADCY9, PHKB, PHKG2, PRKACA, PRKACB</i>	0.0167367
	hsa04911: Insulin secretion	5	1.96E-05	<i>ADCY4, ADCY9, PRKACA, RAPGEF4, PRKACB</i>	0.0198237
	hsa04713: Circadian entrainment	5	3.05E-05	<i>ADCY4, ADCY9, PRKACA, PRKACB, RASD1</i>	0.0308047
	hsa04913: Ovarian steroidogenesis	4	.0001164	<i>ADCY4, ADCY9, PRKACA, PRKACB</i>	0.1174204
	hsa04261: Adrenergic signaling in cardiomyocytes	5	.0001641	<i>ADCY4, ADCY9, PRKACA, RAPGEF4, PRKACB</i>	0.16546
	hsa04923: Regulation of lipolysis in adipocytes	4	.0001737	<i>ADCY4, ADCY9, PRKACA, PRKACB</i>	0.1751419
	hsa04976: Bile secretion	4	.0003232	<i>ADCY4, ADCY9, PRKACA, PRKACB</i>	0.325689
	hsa04918: Thyroid hormone synthesis	4	.0003373	<i>ADCY4, ADCY9, PRKACA, PRKACB</i>	0.3398419
	hsa04971: Gastric acid secretion	4	.0003818	<i>ADCY4, ADCY9, PRKACA, PRKACB</i>	0.384664
	hsa04024: cAMP signaling pathway	5	.0005178	<i>ADCY4, ADCY9, PRKACA, RAPGEF4, PRKACB</i>	0.5212951
	hsa04925: Aldosterone synthesis and secretion	4	.0005188	<i>ADCY4, ADCY9, PRKACA, PRKACB</i>	0.5223062
	hsa04727: GABAergic synapse	4	.0005188	<i>ADCY4, ADCY9, PRKACA, PRKACB</i>	0.5223062
	hsa04970: Salivary secretion	4	.0005773	<i>ADCY4, ADCY9, PRKACA, PRKACB</i>	0.5810495
	hsa05414: Dilated cardiomyopathy	4	.0005773	<i>ADCY4, ADCY9, PRKACA, PRKACB</i>	0.5810495
	hsa04914: Progesterone-mediated oocyte maturation	4	.0006399	<i>ADCY4, ADCY9, PRKACA, PRKACB</i>	0.6438567
	hsa04540: Gap junction	4	.0006617	<i>ADCY4, ADCY9, PRKACA, PRKACB</i>	0.6657144
	hsa04912: GnRH signaling pathway	4	.0007299	<i>ADCY4, ADCY9, PRKACA, PRKACB</i>	0.7341095
	hsa05032: Morphine addiction	4	.0007299	<i>ADCY4, ADCY9, PRKACA, PRKACB</i>	0.7341095
	hsa04750: Inflammatory mediator regulation of TRP channels	4	.0008794	<i>ADCY4, ADCY9, PRKACA, PRKACB</i>	0.8839462
	hsa04723: Retrograde endocannabinoid signaling	4	.0008794	<i>ADCY4, ADCY9, PRKACA, PRKACB</i>	0.8839462
	hsa04922: Glucagon signaling pathway	4	.0009333	<i>PHKB, PHKG2, PRKACA, PRKACB</i>	0.9378678
	hsa04915: Estrogen signaling pathway	4	.0009333	<i>ADCY4, ADCY9, PRKACA, PRKACB</i>	0.9378678
	hsa04916: Melanogenesis	4	.000961	<i>ADCY4, ADCY9, PRKACA, PRKACB</i>	0.9655907
	hsa04114: Oocyte meiosis	4	.0012343	<i>ADCY4, ADCY9, PRKACA, PRKACB</i>	1.2385867
	hsa04725: Cholinergic synapse	4	.001301	<i>ADCY4, ADCY9, PRKACA, PRKACB</i>	1.3051434
	hsa05166: HTLV-I infection	5	.0013669	<i>ADCY4, ADCY9, XBP1, PRKACA, PRKACB</i>	1.3709053
	hsa04724: Glutamatergic synapse	4	.0014053	<i>ADCY4, ADCY9, PRKACA, PRKACB</i>	1.4091087
	hsa04270: Vascular smooth muscle contraction	4	.0015906	<i>ADCY4, ADCY9, PRKACA, PRKACB</i>	1.5936033
	hsa04611: Platelet activation	4	.0019617	<i>ADCY4, ADCY9, PRKACA, PRKACB</i>	1.9620717
	hsa04910: Insulin signaling pathway	4	.0024331	<i>PHKB, PHKG2, PRKACA, PRKACB</i>	2.428359
	hsa04962: Vasopressin-regulated water reabsorption	3	.0033005	<i>ADCY9, PRKACA, PRKACB</i>	3.2811996
	hsa04742: Taste transduction	3	.0034537	<i>ADCY4, PRKACA, PRKACB</i>	3.4310789
hsa04921: Oxytocin signaling pathway	4	.0035747	<i>ADCY4, ADCY9, PRKACA, PRKACB</i>	3.549344	
hsa04961: Endocrine and other factor-regulated calcium reabsorption	3	.0036101	<i>ADCY9, PRKACA, PRKACB</i>	3.583959	
hsa05110: <i>Vibrio cholerae</i> infection	3	.0049786	<i>ADCY9, PRKACA, PRKACB</i>	4.9119684	
hsa04062: Chemokine signaling pathway	4	.0055702	<i>ADCY4, ADCY9, PRKACA, PRKACB</i>	5.4809168	
hsa05200: Pathways in cancer	4	.0418894	<i>ADCY4, ADCY9, PRKACA, PRKACB</i>	35.06845	
Module2	hsa03050: Proteasome	9	5.89E-14	<i>PSMA2, PSM14, PSMA5, PSME2, PSMC2, PSMA4, PSMA3, PSMB2, PSMB9</i>	4.88E-11
Module3	hsa03040:Spliceosome	11	1.18E-15	<i>NCBP2, HNRNPA3, PLRG1, LSM8, RBM8A, LSM6, SNRPD1, LSM5, SNRNP40, LSM2, SF3B4</i>	5.33E-13
	hsa03015: mRNA surveillance pathway	5	1.78E-05	<i>NCBP2, UPF1, RBM8A, NUDT21, SMG7</i>	0.0077335
	hsa03018: RNA degradation	4	.000354	<i>LSM8, LSM6, LSM5, LSM2</i>	0.153867
Module4	hsa03013: RNA transport	3	.0399075	<i>NCBP2, UPF1, RBM8A</i>	16.231928
	hsa03010: Ribosome	9	1.66E-14	<i>MRPL13, MRPL3, MRPS18C, MRPL15, MRPL27, MRPL16, MRPS10, MRPS21, MRPL30</i>	1.65E-12
Module5	hsa03030: DNA replication	6	1.32E-09	<i>PRIM1, POLE2, MCM3, RPA4, FEN1, RPA3</i>	9.35E-07
	hsa03460: Fanconi anemia pathway	5	9.89E-07	<i>PMS2, ERCC4, RPA4, RAD51, RPA3</i>	0.0007024
	hsa03420: Nucleotide excision repair	4	4.72E-05	<i>POLE2, ERCC4, RPA4, RPA3</i>	0.0335351
	hsa03430: Mismatch repair	3	.0005755	<i>PMS2, RPA4, RPA3</i>	0.407984
	hsa03440: Homologous recombination	3	.0009188	<i>RPA4, RAD51, RPA3</i>	0.6506143
	hsa04110: Cell cycle	3	.0158865	<i>ORC5, MCM3, ORC3</i>	10.749309
	hsa03410: Base excision repair	2	.0499469	<i>POLE2, FEN1</i>	30.500744
Module6	hsa03060: Protein export	5	3.07E-08	<i>SRP54, SRP68, SPCS1, SPCS2, SRP9</i>	9.65E-06
	hsa03010: Ribosome	6	1.09E-06	<i>RPL23, RPL15, RPL8, RPL24, RPL11, RPL12</i>	0.0003417

(continued)

Table 3
(continued).

Module ID	Pathway term	Gene count	P	Genes	FDR
Module7	hsa04080: Neuroactive ligand–receptor interaction	4	.0011741	<i>BDKRB1, NPFFR1, GHSR, NTSR2</i>	0.8622339
Module9	hsa04630: Jak-STAT signaling pathway	7	2.12E-09	<i>IL5, IL7, JAK2, SOCS5, IFNGR2, IL11, EPO</i>	1.79E-06
	hsa04060: Cytokine-cytokine receptor interaction	5	7.49E-05	<i>IL5, IL7, IFNGR2, IL11, EPO</i>	0.0631994
Module11	hsa04640: Hematopoietic cell lineage	4	9.70E-05	<i>IL5, IL7, IL11, EPO</i>	0.0818866
	hsa04141: Protein processing in endoplasmic reticulum	2	.0478851	<i>SEC31A, SAR1B</i>	14.312831
Module13	hsa00190: Oxidative phosphorylation	5	1.33E-07	<i>NDUFA4, COX11, COX7C, COX6B1, COX6C</i>	6.84E-05
	hsa05012: Parkinson disease	4	3.38E-05	<i>NDUFA4, COX7C, COX6B1, COX6C</i>	0.0174037
	hsa04932: Nonalcoholic fatty liver disease (NAFLD)	4	3.90E-05	<i>NDUFA4, COX7C, COX6B1, COX6C</i>	0.0201109
	hsa05010: Alzheimer disease	4	5.59E-05	<i>NDUFA4, COX7C, COX6B1, COX6C</i>	0.0288317
	hsa05016: Huntington's disease	4	8.22E-05	<i>NDUFA4, COX7C, COX6B1, COX6C</i>	0.0423499
Module14	hsa04260: Cardiac muscle contraction	3	.0006915	<i>COX7C, COX6B1, COX6C</i>	0.3559762
	hsa01100: Metabolic pathways	5	.0009689	<i>NDUFA4, COX11, COX7C, COX6B1, COX6C</i>	0.4984845
	hsa04070: Phosphatidylinositol signaling system	6	3.12E-09	<i>MTMR3, MTMR1, PIK3R5, PI4K2B, INPP5B, PIP4K2B</i>	3.25E-06
	hsa00562: Inositol phosphate metabolism	5	1.44E-07	<i>MTMR3, MTMR1, PI4K2B, INPP5B, PIP4K2B</i>	0.0001506
	hsa04918: Thyroid hormone synthesis	2	.0497836	<i>CREB1, ATP1A1</i>	38.432176
Module19	hsa00190: Oxidative phosphorylation	5	1.33E-07	<i>NDUF5, NDUFB8, NDUFA9, NDUFA12, NDUFB1</i>	6.35E-05
Module20	hsa05012: Parkinson disease	5	1.73E-07	<i>NDUF5, NDUFB8, NDUFA9, NDUFA12, NDUFB1</i>	8.28E-05
	hsa04932: Nonalcoholic fatty liver disease (NAFLD)	5	2.10E-07	<i>NDUF5, NDUFB8, NDUFA9, NDUFA12, NDUFB1</i>	0.0001005
	hsa05010: Alzheimer disease	5	3.41E-07	<i>NDUF5, NDUFB8, NDUFA9, NDUFA12, NDUFB1</i>	0.0001632
	hsa05016: Huntington disease	5	5.72E-07	<i>NDUF5, NDUFB8, NDUFA9, NDUFA12, NDUFB1</i>	0.0002739
	hsa01100: Metabolic pathways	5	.0009689	<i>NDUF5, NDUFB8, NDUFA9, NDUFA12, NDUFB1</i>	0.4628423

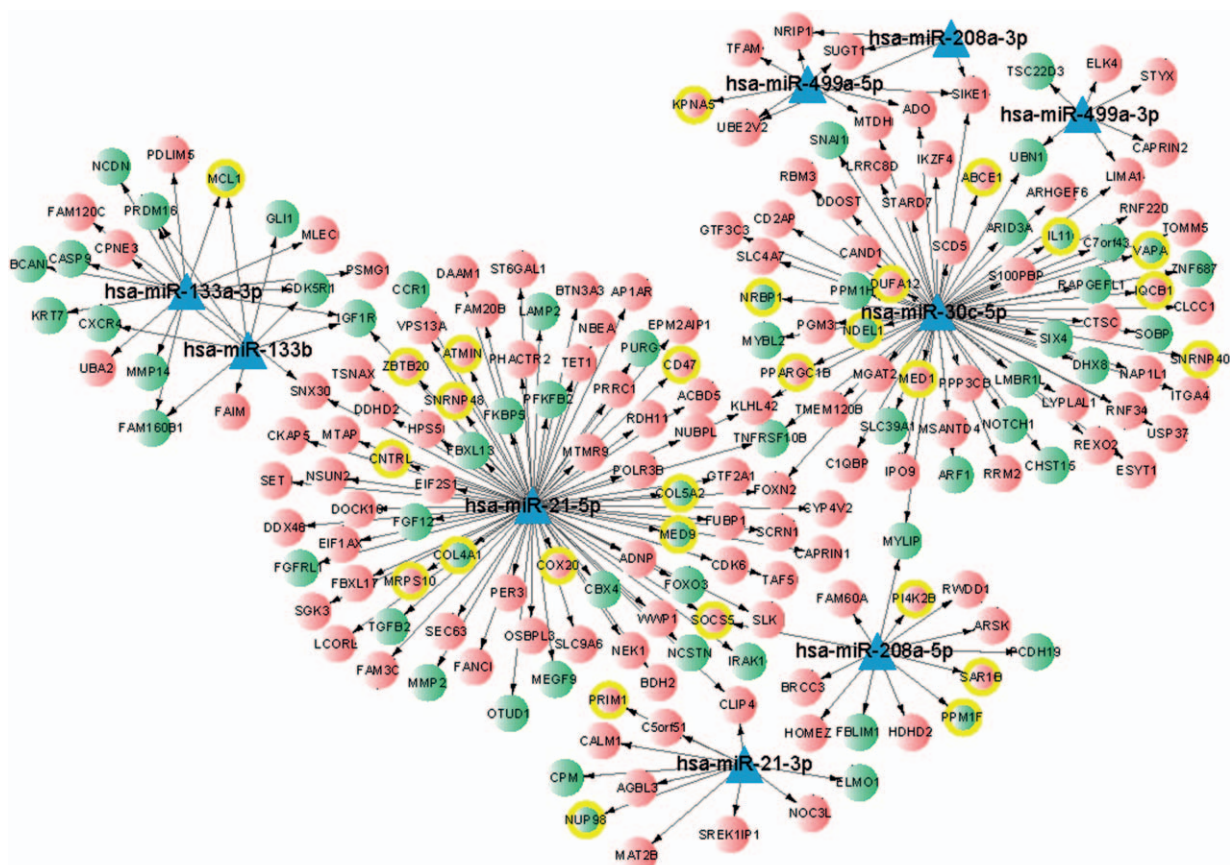


Figure 3. A microRNA-gene network consisting of differentially expressed genes and the miRNAs regulating them, A, triangle represents a microRNA, B, a circle represents a differentially expressed gene.

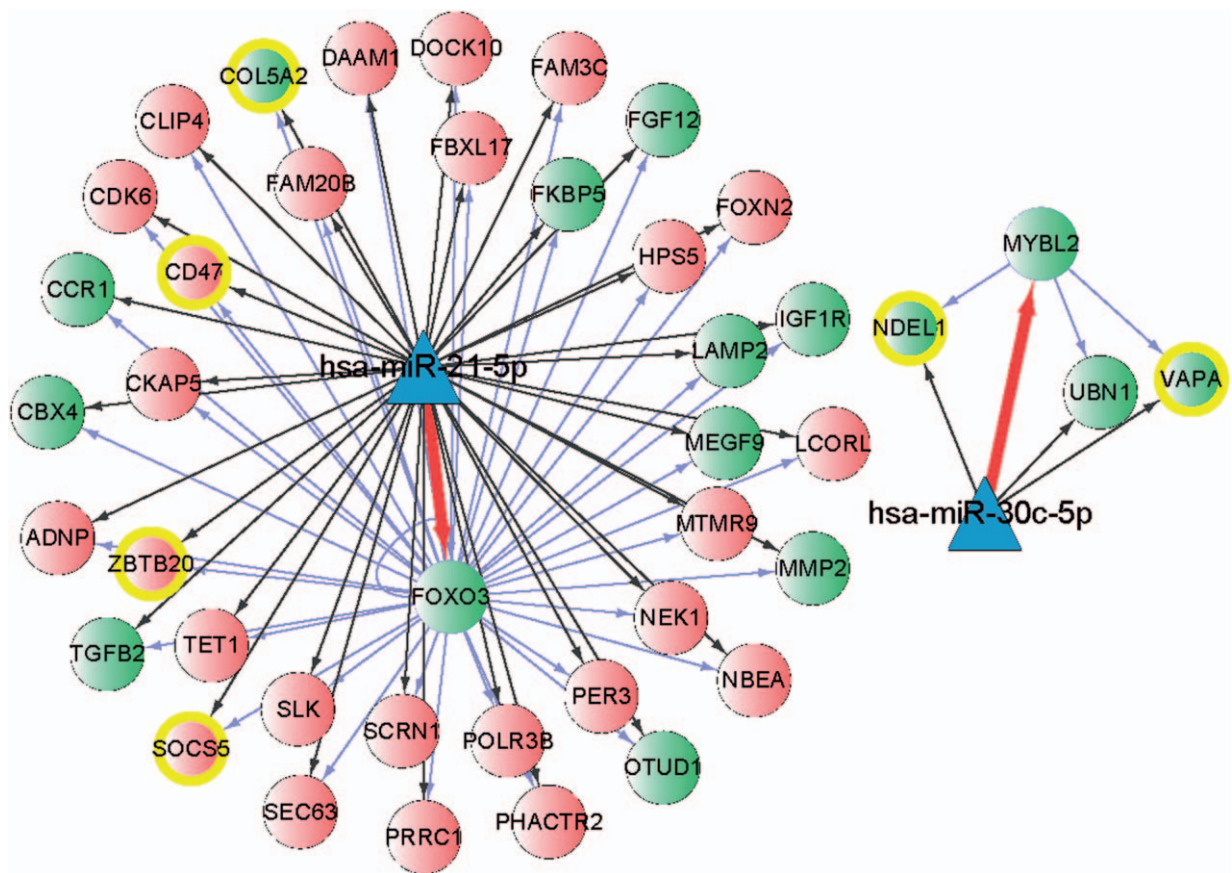


Figure 4. The transcription factor-miRNA-gene network, A, triangle represents a microRNA, B, green circle represents the upregulated differentially expressed gene or upregulated transcription factor, and red circle represents the downregulated differentially expressed gene.

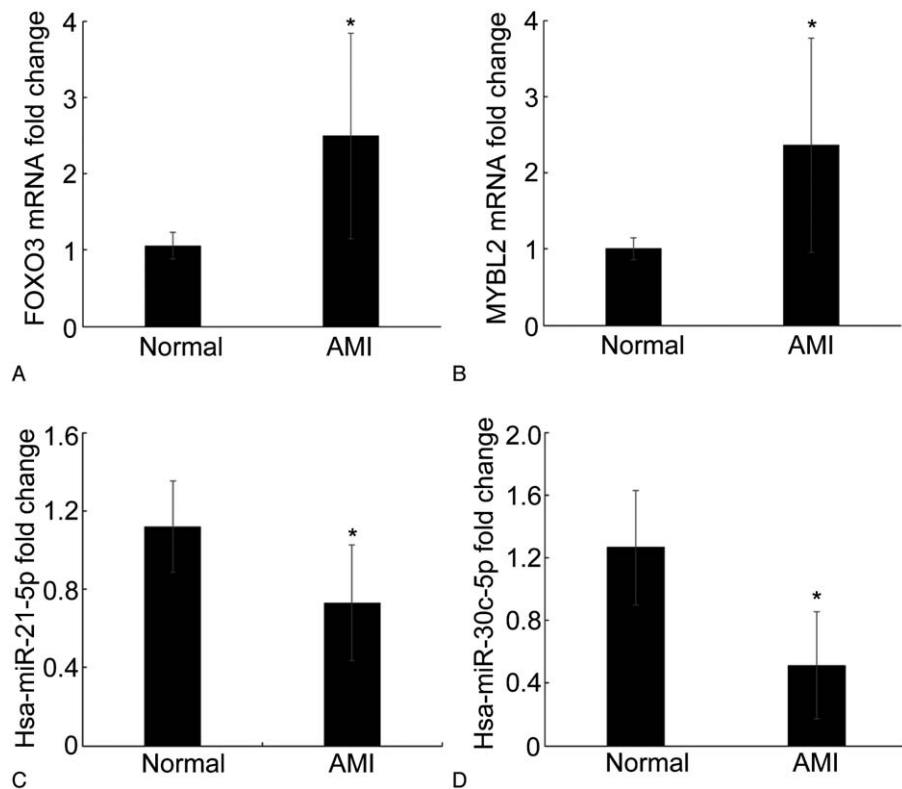


Figure 5. Expression levels of *FOXO3*, *MYBL2*, *hsa-miR-21-5p*, and *hsa-miR-30c-5p* determined using quantitative real-time PCR.

COL5A2 expression. Previously, Dong et al^[27] reported that miR-21 expression was significantly decreased in infarcted areas of rat hearts 6 hours after AMI. Dong et al^[27] have confirmed that miR-21 has a protective effect against cardiac cell apoptosis via its target gene *PDCD4* in the early phase of AMI. An elevated expression of hsa-miR-21-5p was also identified in this study. Thus, hsa-miR-21-5p may also be involved in AMI via regulating various DEGs, such as *SOCS3* and *COL5A2*.

VAPA encoding vesicle-associated membrane protein associated protein-A showed an upregulated expression in AMI patients here. According to the previously published literatures, *VAPA* is commonly involved in the regulation of endoplasmic reticulum to Golgi transportation via binding to oxysterol-binding protein, by which to regulate vesicle transport and sterol homeostasis.^[28–30] However, the biofunction of *VAPA* in AMI is rarely reported, and only Zhao et al^[31] have reported that *VAPA* is markedly decreased in the infarcted myocardium of rats, which is contrary to our identification. Therefore, further investigation of *VAPA* in AMI was still required. Here, *VAPA* expression was predicated to be regulated by *MYBL2* and *hsa-miR-30c-5p*. *MYBL2* encodes a member of the MYB family member Myb-related protein B. Increased *MYBL2* expression was reported in the peripheral blood leukocytes of humans with acute ischemic stroke^[32] and it is also implicated to participate in the regulation of genes downregulated in left ventricular remodeling following myocardial infarction.^[33] Taken together, *VAPA* upregulation observed here may be elevated by transcription factor *MYBL2*. Hsa-miR-30c-5p has been reported as an apoptosis-related microRNA in myocardial infarction.^[34] Duisters et al^[35] further reported that miR-30 directly downregulated connective tissue growth factor (CTGF), which thus was considered to have an important role in the control of structural changes in the extracellular matrix of the myocardium, which was consistent with the result validated in this study. Thus, this miRNA may perform an adverse effect in the regulation of *VAPA* expression in AMI. Another 2 upregulated genes *UBN1* and *NDEL1* were also speculated to be regulated by *MYBL2* and *hsa-miR-30c-5p*. *UBN1* encodes the shutting protein ubinuclein 1, which was an interacting partner of *RACK1* protein, and the latter is confirmed to have a role in the process of myocardial damage.^[36] Thus, we assume that *UBN1* may be involved in the pathogenesis of AMI. However, *NDEL1* encoding a thiol-activated oligopeptidase that is involved in the regulation of cytoplasmic dynein function and microtubule organization during mitotic cell division has never been reported in AMI.

However, there were also some limitations that should be strengthened in this study. First, because most of the results in this study were obtained from in silico analysis, thus, further experimental validations should be required. Second, although expression levels of several DEGs and predicted miRNA were verified to be consistent with the bioinformatic analysis results, the regulatory ships between them were still not be confirmed, as well as the enrichment analytical results. Third, some of the results identified in this study were not consistent with previously published results in other diseases. Therefore, further validations in both in vivo and in vitro were still needed. Despite these limitations, our study also provided some new insights in the mechanism of AMI.

In summary, we identified 41 DEGs, such as *SOCS3*, *VAPA*, and *COL5A2*, that were speculated to have a role in the pathogenesis of AMI, as well as 2 transcription factors *FOXO3* and *MYBL2*, and 2 miRNAs hsa-miR-21-5p and hsa-miR-30c-5p that might regulate the expression of these DEGs. Our work

provides some potential genes for the targeted therapy of AMI and its early detection. However, as some of our findings are not consistent with the published references, we have to further validate them by other means.

References

- Granger CB, Califf RM, Topol EJ. Thrombolytic therapy for acute myocardial infarction. *Drugs* 1992;44:293–325.
- Aversano T, Aversano LT, Passamani E, et al. Thrombolytic therapy vs primary percutaneous coronary intervention for myocardial infarction in patients presenting to hospitals without on-site cardiac surgery: a randomized controlled trial. *JAMA* 2002;287:1943–51.
- Eagle KA, Goodman SG, Avezum A. Practice variations and missed opportunities for reperfusion in ST-segment elevation myocardial infarction: findings from the Global Registry of Acute Coronary Events (GRACE) ☆. *Lancet* 2002;11:16.
- Cohen M, Gensini GF, Maritz F, et al. Prospective evaluation of clinical outcomes after acute ST-elevation myocardial infarction in patients who are ineligible for reperfusion therapy: preliminary results from the TETAMI registry and randomized trial. *Circulation* 2003;108:14–21.
- Keller T, Zeller T, Peetz D, et al. Sensitive troponin I assay in early diagnosis of acute myocardial infarction. *N Engl J Med* 2009;361:868–77.
- Roppolo LP, Fitzgerald R, Dillow J, et al. A comparison of troponin T and troponin I as predictors of cardiac events in patients undergoing chronic dialysis at a Veteran's Hospital: a pilot study. *J Am Coll Cardiol* 1999;34:448–54.
- Mccann CJ, Glover BM, Menown IB, et al. Novel biomarkers in early diagnosis of acute myocardial infarction compared with cardiac troponin T. *Eur Heart J* 2008;29:2843–50.
- Adachi T, Nakanishi M, Otsuka Y, et al. Plasma microRNA 499 as a biomarker of acute myocardial infarction. *Clin Chem* 2010;56:1183–5.
- Wang GK, Zhu JQ, Zhang JT, et al. Circulating microRNA: a novel potential biomarker for early diagnosis of acute myocardial infarction in humans. *Eur Heart J* 2010;31:659–66.
- Ai J, Zhang R, Li Y, et al. Circulating microRNA-1 as a potential novel biomarker for acute myocardial infarction. *Biochem Biophys Res Commun* 2010;391:73–7.
- Carvalho B, Bengtsson H, Speed TP, et al. Exploration, normalization, and genotype calls of high-density oligonucleotide SNP array data. *Biostatistics* 2007;8:485–99.
- Huang da W, Sherman BT, Lempicki RA. Systematic and integrative analysis of large gene lists using DAVID bioinformatics resources. *Nat Protoc* 2008;4:44–57.
- Wu G, Dawson E, Duong A, et al. ReactomeFIViz: a Cytoscape app for pathway and network-based data analysis. *F1000Res* 2014;3:146–246.
- Shannon P, Markiel A, Ozier O, et al. Cytoscape: a software environment for integrated models of biomolecular interaction networks. *Genome Res* 2003;13:2498–504.
- Dweep H, Gretz N. miRWalk2.0: a comprehensive atlas of microRNA-target interactions. *Nat Methods* 2015;12:697.
- Janky R, Verfaillie A, Imrichová H, et al. iRegulon: from a gene list to a gene regulatory network using large motif and track collections. *PLoS Comput Biol* 2014;10:e1003731.
- Terrell AM, Crisostomo PR, Wairiuko GM, et al. Jak/STAT/SOCS signaling circuits and associated cytokine-mediated inflammation and hypertrophy in the heart. *Shock* 2006;26:226–34.
- Shi J, Wei L. Regulation of JAK/STAT signalling by SOCS in the myocardium. *Cardiovasc Res* 2012;96:345–7.
- Seki YI, Hayashi K, Matsumoto A, et al. Expression of the suppressor of cytokine signaling-5 (SOCS5) negatively regulates IL-4-dependent STAT6 activation and Th2 differentiation. *Proc Natl Acad Sci U S A* 2002;99:13003–8.
- Linossi EM, Chandrashekar IR, Kolesnik TB, et al. Suppressor of Cytokine Signaling (SOCS) 5 utilizes distinct domains for regulation of JAK1 and interaction with the adaptor protein Shc-1. *PLoS One* 2013;8:e70536.
- Toghi M, Taheri M, Arsang-Jang S, et al. SOCS gene family expression profile in the blood of multiple sclerosis patients. *J Neurol Sci* 2017;375:481.
- Zhang S, Liu X, Goldstein S, et al. Role of the JAK/STAT signaling pathway in the pathogenesis of acute myocardial infarction in rats and its effect on NF- κ B expression. *Mol Med Rep* 2013;7:93–8.

- [23] Azuaje F, Lu Z, Jeanty C, et al. Analysis of a gene co-expression network establishes robust association between Col5a2 and ischemic heart disease. *BMC Med Genomics* 2012;6:1988–94.
- [24] Wang Y, Lin W, Li C, et al. Multipronged therapeutic effects of Chinese herbal medicine Qishenyiqi in the treatment of acute myocardial infarction. *Front Pharmacol* 2017;8:98.
- [25] Evans-Anderson HJ, Alfieri CM, Yutzey KE. Regulation of cardiomyocyte proliferation and myocardial growth during development by FOXO transcription factors. *Circ Res* 2008;102:686–94.
- [26] Sengupta A, Molkentin JD, Paik JH, et al. FoxO transcription factors promote cardiomyocyte survival upon induction of oxidative stress. *J Biol Chem* 2011;286:7468–78.
- [27] Dong S, Cheng Y, Yang J, et al. MicroRNA expression signature and the role of microRNA-21 in the early phase of acute myocardial infarction. *J Biol Chem* 2009;284:29514–25.
- [28] Prosser DC, Tran D, Gougeon PY, et al. FFAT rescues VAPA-mediated inhibition of ER-to-Golgi transport and VAPB-mediated ER aggregation. *J Cell Sci* 2008;121:3052–61.
- [29] Wyles JP, McMaster CR, Ridgway ND. Vesicle-associated membrane protein-associated protein-A (VAP-A) interacts with the oxysterol-binding protein to modify export from the endoplasmic reticulum. *J Biol Chem* 2002;277:29908–18.
- [30] Weber-Boyvat M, Kentala H, Lilja J, et al. OSBP-related protein 3 (ORP3) coupling with VAMP-associated protein A regulates R-Ras activity. *Exp Cell Res* 2015;331:278–91.
- [31] Zhao W, Zhao T, Chen Y, et al. Modification of oxidative stress on gene expression profiling in the rat infarcted heart. *Mol Cell Biochem* 2013;379:243–53.
- [32] Yan J, Liu J, Greer JM, et al. Increased expression of the hypoxia-related genes in peripheral blood leukocytes of human subjects with acute ischemic stroke. *Clin Exp Neuroimmunol* 2014;5:216–26.
- [33] Kuster DWD, Merkus D, Kremer A, et al. Left ventricular remodeling in swine after myocardial infarction: a transcriptional genomics approach. *Basic Res Cardiol* 2011;106:1269–81.
- [34] Liu Q, Du GQ, Zhu ZT, et al. Identification of apoptosis-related microRNAs and their target genes in myocardial infarction post-transplantation with skeletal myoblasts. *J Transl Med* 2015; 13:1–1.
- [35] Duisters RF, Tijssen AJ, Schroen B, et al. miR-133 and miR-30 regulate connective tissue growth factor implications for a role of microRNAs in myocardial matrix remodeling. *Circ Res* 2009;104:170–261.
- [36] Jia X, Zhang L, Mao X. S-propranolol protected H9C2 cells from ischemia/reperfusion-induced apoptosis via downregulation of RACK1 gene. *Int J Clin Exp Pathol* 2015;8:10335–44.